Annals of Phytomedicine 13(1): 495-506, 2024

DOI: http://dx.doi.org/10.54085/ap.2024.13.1.51

Annals of Phytomedicine: An International Journal
http://www.ukaazpublications.com/publications/index.php

Print ISSN : 2278-9839 Online ISSN : 2393-9885

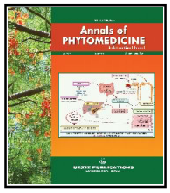

Original Article : Open Access

Sesquiterpene coumarins of Asafoetida mask the functional site of pathogenic proteins of SARS-CoV-2 to combat COVID-19 disease

Surekha Ramachandran◆
Department of Biochemistry, SRM Dental College, Bharathi Salai, Ramapuram, Chennai-600089, Tamil Nadu, India

Article Info

Article history
Received 13 March 2024
Revised 27 April 2024
Accepted 28 April 2024
Published Online 30 June 2024

Keywords
SARS-CoV-2
COVID-19
Asafoetida
ADMET
Molecular docking

Abstract

The rapid unexpected spread of the symptoms of novel SARS coronavirus (SARS-CoV-2) sets an alarm for developing drugs to cure COVID-19. Targeting the mechanism of virus infection through the host cell recognition was considered a key factor in drug development. In the present study, a traditional spice, asafoetida was used, where an initial selection of compounds on PASS analysis revealed that the sesquiterpene coumarins of asafoetida; namely, foetidin, umbelliferone, gummosin, conferol, assafoetidnol A, and galbanic acid showed an extensive probability of drug to be active. ADMET experiment showed a desirable physicochemical potency of coumarins, and it is considered safe for human consumption. Autodock analysis demonstrated the binding relationship of selected drugs with the infectious proteins of SARS-CoV-2, where the selected compounds showed a stable dock score and increased binding interaction. Galbanic acid exhibited a potential non-covalent interaction with proteins such as ACE2 receptor, papain protease, and RNA polymerase. Assafoetidnol A occupies the receptor-binding site of spike glycoprotein and the catalytic site of papain protease to block viral attachment and multiplication, respectively. Conferol, foetidin, and umbelliferone also displayed a stable interaction with the target proteins. The result of the docking parameters was further compared with the reference standard, hydroxychloroquine to understand the potency of the selected compounds. In conclusion, the coumarins of asafoetida might selectively interact and modify the pathogenic polypeptides of SARS-CoV-2 to inhibit the contagious disease mechanism of COVID-19.

1. Introduction

The pandemic outbreak of the zoonotic virus from Wuhan, China set an utmost public health emergency since late 2019 (Song *et al*., 2020). The pandemic infection was termed COVID-19 disease caused duly by SARS-CoV-2, resulting in severe infection with atypical pneumonia (Zhu *et al*., 2020). The novel SARS-CoV-2 exhibited a high rate of recombination that manifests to be more invasive, extremely contagious, and showed a greater extent of morbidity, and mortality than SARS-CoV (Petersen *et al*., 2020). Increased virus load aggravates the symptoms of COVID-19 ranging from high temperature, common cold, acute respiratory disorders, shortness of breath, chemosensory dysfunction, renal failure, and even death (Wang *et al*., 2020).

The enveloped SARS-CoV-2 was found to carry the largest positive-sense single-stranded RNA (ssRNA) genome encoding genes for the structural and non-structural viral components (Fehr and Perlman, 2015). Initially, the virus uses spike (S) protein to enter the bronchial epithelial cells by endocytic pathway by attaching to the receptor angiotensin converting enzyme 2(ACE2). After attachement, S protein undergoes structural changes, exposing its fusogenic domain to encourage fusion with the endosomal membrane to liberate viral ssRNA into the cytoplasm. The ssRNA of virus contains ORF1a and ORF1b at the 5'end of the untranslated region (UTR) which was then translated by the host cell ribosomes into polyproteins. It was further cleaved at distinct sites by the cysteinyl proteases or main protease (M^{pro}) to promote gene expression, maturation, and replication (Kumar *et al*., 2020).

The viral structure and life cycle are very subtle and intricate (Naqvi *et al*., 2020). Several research being conducted globally to develop a potent antiviral medicine to target the pathophysiology of SARS-CoV-2 infection (Samaddar *et al*., 2020; Trougakos *et al*., 2021). Most of the drugs under investigation target protease activity to curb the virus cell multiplication and assembly (Caly *et al*., 2020; Poduri *et al*., 2020). In addition, the virus spike glyocprotein of SARS-CoV-2 also remains as a successful target for the drug and vaccine development. Therefore, in this study, the capsid protein and enzymes responsible for gene expression and assembly are targeted using molecular docking analysis. The docking parameter is one of the most preferred SBDD strategy to provide insight into the development of drugs by targeting the active site or specific site of functional protein with the highest degree of accuracy (Kalyaanamoorthy and Chen, 2011).

Asafoetida is a gum resin extracted from *Ferula asafoetida* plant stem which has a strong and sulfurous odor used as a traditional spice in Indian cuisine for centuries (Shahrajabian *et al*., 2021). Asafoetida renders effective remedies against whooping cough, lung disorders, gastro-intestinal disturbances, flatulence, and intestinal parasitic infection. The phytochemistry of asafoetida found to contain various active components including sesquiterpene coumarins, sulfur-containing compounds, monoterpenes, terpenoids, coumarins, esters,

Corresponding author: Dr. Surekha Ramachandran
Department of Biochemistry, SRM Dental College, Bharathi Salai, Ramapuram, Chennai-600089, Tamil Nadu, India
E-mail: rsurekha2013@gmail.com
Tel.: +91-9940186459

polysaccharides, and glycoproteins which reveal several pharmacological activities including antioxidant, antimicrobial, antiviral, antifungal, antidiabetic, anticarcinogenic, neuroprotective, antispasmodic, and hypotensive properties (Amalraj and Gopi, 2016; Mahendra and Bisht, 2012). Based on the broad medicinal applications of asafoetida, the present study was framed to assess the antiviral potency against SARS-CoV-2. Thus, the study objective was framed to determine the key compounds of asafoetida by utilizing virtual screening and ADME/toxicity predictions. Subsequently, the study aimed to examine the docking interactions between these principal compounds of asafoetida and the functional sites of target proteins of SARS-CoV-2.

2. Materials and Methods

2.1 Pharmacodynamic study

A pharmacodynamic study was carried out using the PASS online server. PASS software uses the structure of an organic compound to predict the biological activity of drug-like molecules (Poroikov *et al*., 2003).

2.2 ADMET properties

ADME (adsorption, distribution, metabolism, and excretion) properties were predicted virtually by accessing freely available SwissADME software to analyze solubility, lipophilicity, intestinal bio-absorption, BBB permeability, and cytochrome P450 inhibition (Diana *et al*., 2017). The compounds of asafoetida resins were screened selectively for the applications of drug likeliness by evaluating the compounds to follow Rule of 5. The Rule of 5 explains physicochemical and structural properties within certain ranges to signify active compounds for oral consumption (Lipinski *et al*., 2001). Further, the toxic nature of the compounds was determined with the online pkCSM software to improve compound quality and success rate. The toxicity mode was selected and the toxicity effects such as the maximum tolerated dose by humans and lethal dose for rats (LD_{50}) were analyzed and tabulated (Pires *et al*., 2015). The compounds with valid pharmacodynamic characteristics and ADMET properties were listed and used for computational docking analysis.

2.3 Molecular docking interaction analysis Analysis

The Autodock 4.2.6 software was used to conduct computational docking investigation.

2.3.1 Ligand preparation

The active components from asafoetida resin were screened to perform the molecular docking analysis. Hydroxychloroquine was used a reference standard. The three-dimensional structures of sesquiterpene coumarins and hydroxychloroquine were downloaded from PubChem database in SDF format. Then the SDF files were later converted into the PDB file format using BIOVIA Discovery Studio (Accelrys, 2018).

2.3.2 Target preparation

The structure of SARS-COV-2 S-glycoprotein RBD (6Z97), human ACE-2 receptor (6VW1), main protease (6XCH), papain protease (7JRN), and RNA-dependent RNA polymerase (RdRp) (7BW4) were retrieved from Protein Data Bank (http://www.rscb.org) with good resolution. Tahir ul Qamar *et al.* (2020) and Tariq *et al.* (2020) demonstrated the catalytic active site residues of pathogenic proteins of SARS-CoV-2, which was listed in Table 1. In this study, the molecular docking parameters were performed by targeting the amino acid sequences present in the functional active site of each protein. For the target-ligand interaction, the water molecules, inhibitors, and ions present in active sites were eliminated and saved the target molecule in PDB file format using BIOVIA Discovery Studio (Accelrys, 2018).

Table 1: Functional site/catalytic site residues of target proteins

S.No.	Target protein of SARS-CoV-2	Binding site residues
1.	Spike glycoprotein RBD domain	Arg403, Asp405, Glu406, Arg408, Gln409, Thr415, Gly416, Lys417, Asp420, Tyr421, Tyr449, Tyr453, Phe456, Phe490, Gln493, Ser494, Tyr495, Gly496, Phe497, Asn501, Gly502, Val503, Gly504, Tyr505
2.	ACE2 receptor	Gln24, Thr27, Phe28, Asp30, Lys31, His34, Glu35, Glu37, Asp38, Tyr41, Gln42, Ser44, Leu79, Met82, Tyr83, Asn330, Lys353, Gly354, Asp355, Arg357, Arg393
3.	Main protease	Thr24, Thr25, Thr26, Leu27, His41, Cys44, Thr45, Ser46, Met49, Phe140, Leu141, Asn142, Gly143, Ser144, Cys145, His163, His164, Met165, Glu166, Leu167, Pro168, Asp187, Arg188, Gln189, Thr190, Gln192
4.	Papain protease	Asp164, Val165, Arg166, Glu167, Met208, Cys217, Ala246, Pro247, Pro248, Tyr264, Gly266, Asn267, Tyr268, Gln269, Gly271, Tyr273, Thr301, Asp302
5.	RNA dependent RNA polymerase	Phe429, Lys430, Glu431, Gly432, Ser433, Glu436, Leu437, Lys438, His439, Phe440, Phe441, Phe442, Asp452, Tyr455, Tyr456, Ile494, Asn496, Asn497, Asp499, Thr540, Gln541, Met542, Ser549, Ala550, Lys551, Arg553, Gly559, Thr565, Asn568, Arg569, His572, Gln573, Leu576, Lys577, Ala580, Arg583, Val588, Ile589, Gly590, Thr591, Ser592, Lys593, Phe594, Trp598, Asn600, Pro620, Lys621, Cys622, Asp623, Arg624, Thr686, Thr687, Ala688, Tyr689, Asn691

2.3.3 Grid preparation and docking analysis

The docking parameters of the target protein were generated by removing all nonpolar hydrogens leaving the polar and the charged ones and saved as PDBQT. Further in each ligand, the Kollman charges were assigned, and rotatable bonds were detected and saved as PDBQT. The functional site of each protein was selected by choosing the suitable grid box coordinates which was given in Table 2. Ligand and the target protein were docked by validating the Lamarckian genetic algorithm (GA) parameters and empirical force field to output

10 conformational binding energy scores (Sumathi and Vidhya, 2022). The hydrogen bond (intermolecular) interaction formed between the ligand and amino acid residues of each protein were visualized using BIOVIA Discovery Studio (Accelrys, 2018).

Table 2: Grid box dimensions

Target protein	Grid box dimensions (Å)			Grid box size		
	X	Y	Z	X	Y	Z
Spike glycoprotein	19.861	-12.667	-50.222	60	60	60
ACE2 receptor	13.417	-9.472	-5.944	60	60	60
Main protease	-18.694	-1.278	2.639	60	60	60
Papain protease	-3.000	-11.556	10.583	60	60	60
RNA-dependent RNA polymerase	-6.278	-13.917	3.167	60	60	60

3. Results

3.1 Selection of phytochemicals by PASS program

An initial selection of photo components of asafoetida was done using a PASS computer program. The predicted data carries a list of activity entities with the probability estimation for each type of biological function which was represented as "to be active "Pa" and to be inactive "Pi" and its value ranges from zero to one. The data suggested that the probability of the drug profile being "active" or "inactive" aids an initial selection of compounds that possess antiviral activity against influenza, Herpes, hepatitis B, and HIV (Table 3). Among the various phytoconstituents of asafoetida, the sesquiterpene coumarins; namely, foetidin, umbelliferone, gummosin, conferol, assafoetidnol A, and galbanic acid showed an extensive probability of antiviral, anti-inflammatory, and viral entry inhibitory effects when analyzed using the PASS program, thus the compounds were selected and optimized to display their anti-viral potency against SARS-CoV-2.

Table 3: Pharmacodynamic prediction of phytochemical constituents of asafoetida using PASS online server

Ligands		Viral entry inhibitor	Antiviral	Antiviral (influenza)	Antiviral (Herpes)	Antiviral (hepatitis B)	Antiviral (HIV)	Anti-inflammatory
Foetidin	Pa	0,205	0,187	0,254	0,361	0,207	0,623	0,623
	Pi	0,139	0,109	0,128	0,054	0,081	0,027	0,027
Umbelliferone	Pa	0,237	0,262	0,428	0,439	0,403	0,648	0,648
	Pi	0,053	0,053	0,038	0,021	0,015	0,023	0,023
Gummosin	Pa	0,205	0,188	0,383	0,402	0,260	0,643	0,643
	Pi	0,139	0,108	0,052	0,035	0,046	0,024	0,024
Conferol	Pa	0,205	0,194	0,497	0,435	0,217	0,576	0,576
	Pi	0,139	0,102	0,023	0,022	0,071	0,037	0,037
Assafoetidnol A	Pa	0,237	0,163	0,261	0,393	0,223	0,653	0,653
	Pi	0,053	0,144	0,120	0,038	0,067	0,022	0,022
Galbanic acid	Pa	0,205	0,165	0,221	0,338	0,245	0,524	0,524
	Pi	0,139	0,052	0,089	0,067	0,053	0,050	0,050
Vanillin	Pa	0,237	-	0,257	0,382	0,167	0,135	0,436
	Pi	0,053	-	0,125	0,044	0,141	0,085	0,015
Umbelliprenin	Pa	-	0,164	0,219	0,444	0,191	0,124	0,651
	Pi	-	0,131	0,169	0,020	0,098	0,106	0,023
Isopimpinellin	Pa	-	0,123	-	0,330	0,282	0,126	0,644
	Pi	-	0,102	-	0,072	0,038	0,102	0,024
Terpineol	Pa	0,209	-	-	0,385	0,167	-	0,651
	Pi	0,124	-	-	0,042	0,141	-	0,023
Taraxacin	Pa	0,204	-	-	0,378	0,207	-	0,437
	Pi	0,142	-	-	0,045	0,080	-	0,078

Fetidone A	Pa	0,237	0,263	0,463	-	0,307	0,135	0,641
	Pi	0,052	0,128	0,029	-	0,032	0,085	0,024
Fetidone B	Pa	0,237	0,141	0,571	0,355	-	-	0,606
	Pi	0,053	0,089	0,015	0,057	-	-	0,030
1-(methylthio) propyl 1-propenyl disulfide	Pa	0,237	-	0,256	-	-	0,287	-
	Pi	0,053	-	0,125	-	-	0,010	-
10-epi-g-eudesmol	Pa	-	-	-	0,278	0,287	0,135	0,586
	Pi	-	-	-	0,107	0,037	0,085	0,035
β-Sitosterol	Pa	-	0,145	0,686	0,205	-	0,136	0,467
	Pi	-	0,108	0,006	0,171	-	0,084	0,067
Ferulic acid	Pa	0,328	-	0,501	-	0,046	0,060	0,409
	Pi	0,004	-	0,022	-	0,473	0,149	0,043
Luteolin	Pa	0,243	-	0,462	-	0,006	0,067	-
	Pi	0,043	-	0,030	-	0,046	0,060	-

Pa indicates “Probability of drug to be active”, Pi indicates “Probability of drug to be inactive”.

3.2 Web-based pharmacokinetic ADME study

The phytocompounds of asafoetida were tested for pharmacokinetics proficiency, including human gastrointestinal absorption, BBB permeability, and bioavailability of the drug using SwissADME software. Bioavailability plays an integral part in the pharmacokinetics paradigm which corresponds to drug absorption, effectiveness, and safety. Table 4 showed the bioavailability status of all the phytochemicals of asafoetida. Among the various phytochemicals, the bioavailability score of galbanic acid was found to be a maximum of 0.56 and all the other drugs showed a score of 0.55 favoring the compound as suitable for oral dosing. The selected sesquiterpene coumarins also showed a good agreement with the criteria of Lipinski’s rule without any violation. The present study also revealed that the LogP value of all the ligands under investigation showed a consistent number below 5 (Table 4). The computational prediction of the toxicity prediction was found to be negative with AMES mutagenic test and presented in Table 4 along with the human maximum tolerated dose.

Table 4: ADMET study of phytochemical constituents of asafoetida

Ligands	Water solubility	Lipophilicity consensus (log $P_{o/w}$)	Gastro intestinal (GI) absorption	Blood-brain barrier permeability	P-glycoprotein substrate	Bioavailability score	Lipinski rule (rule of 5)	AMES test	Max. tolerated dose in human (log mg/kg/day)	Oral rat acute toxicity (LD_{50}) (mol/kg)
Foetidin	Poor	4.48	High	Yes	Yes	0.55	Yes	Negative	-0.171	2.546
Umbelliferone	Soluble	1.51	High	Yes	Yes	0.55	Yes	Negative	0.689	2.047
Gummosin	Poor	4.52	High	Yes	Yes	0.55	Yes	Negative	-0.171	2.546
Conferol	Poor	4.42	High	Yes	Yes	0.55	Yes	Negative	-0.447	2.789
Assafoetidnol A	Moderately soluble	3.70	High	No	Yes	0.55	Yes	Negative	-0.447	2.789
Galbanic acid	Poor	4.58	High	No	Yes	0.56	Yes	Negative	0.716	2.526
Vanillin	Soluble	1.20	High	Yes	No	0.55	Yes	Negative	1.285	1.937
Umbelliprenin	Poorly soluble	5.95	High	No	No	0.55	Yes; 1 Violation	Negative	0.497	2.336
Isopimpinellin	Moderately soluble	2.16	High	Yes	No	0.55	Yes	Negative	-0.334	2.142
Terpineol	Soluble	2.58	Low	Yes	No	0.55	Yes	Negative	0.886	1.923
Taraxacin	Soluble	2.18	High	Yes	No	0.55	Yes	Negative	0.21	1.814
Fetidone A	Soluble	2.73	High	Yes	No	0.55	Yes	Negative	0.409	1.795
Fetidone B	Soluble	2.68	High	Yes	No	0.55	Yes	Negative	0.384	1.786

1-(methylthio) propyl 1-propenyl disulfide	Soluble	3.10	Low	Yes	No	0.55	Yes; 1 Violation	Negative	0.571	2.741
10-epi-g-eudesmol	Soluble	3.60	High	Yes	No	0.55	Yes	Negative	0.055	1.681
β-Sitosterol	Poorly soluble	7.19	Low	No	No	0.55	Yes; 1	Negative Violation	-0.621	2.552
Ferulic acid	Soluble	6.36	High	Yes	No	0.55	Yes	Negative	1.082	2.282
Luteolin	Soluble	1.73	High	No	No	0.55	Yes	Negative	0.499	2.455

ADME- Absorption digestion metabolism excretion; AMES test - *Salmonella typhimurium* reverse mutation assay; LD_{50} - Lethal dose at 50 millirems; ADME is predicted using SwissADME software; Toxicity was analyzed by pkCSM software.

3.3 *In silico* analysis of SARS-CoV-2 spike protein

Interruption of receptor-spike protein recognition is considered important to combat virus entry and potential drug design targets. The amino acid sequences of the RBD region of the S protein of SARS-CoV-2 were identified and targeted with sesquiterpene coumarins in the present study. The study highlighted that all the selected coumarins stall the virus entry by irreversibly binding to the RBD of S glycoprotein at varying binding energy (Table 5). Among them, assafoetidnol A displayed a maximum binding affinity (-5.74 kcal/mol) and significant inhibition constant (61.71 µM) with hydrogen and hydrophobic interactions at Arg403, Gln409, Thr415, Lys417 residues of RBD region of spike glycoprotein. Similarly, conferol interacts with the amino acids of RBD of spike protein to interrupt the receptor recognition *via* forming noncovalent bonds at Ser494, Lys417, Tyr453, and Gln493 residues with a binding affinity of -6.05 kcal/mol and inhibition constant of 36.67 µM. Galbanic acid form hydrogen bond interaction at Ser494 and hydrophobic interactions at Arg403 and Glu406 amino acids with a considerable binding affinity (-5.68 kcal/mol) and inhibition constant (68.35 µM). Foetidin also displayed a strong binding affinity and inhibition constant via noncovalent attachment with the residues of RBD of spike protein at Arg403 and Lys417 residues. In the order of binding affinity and bond formation, umbelliferone, and gummosin stand at the end, expressing a marked level of binding affinity via forming remarkable hydrogen and hydrophobic interactions. Further, the standard drug, hydroxychloroquine found to show a stable interaction at Phe490 and Gln493 with a binding affinity of -3.65 kcal/mol and inhibition constant of 196.09 µM (Figure 1).

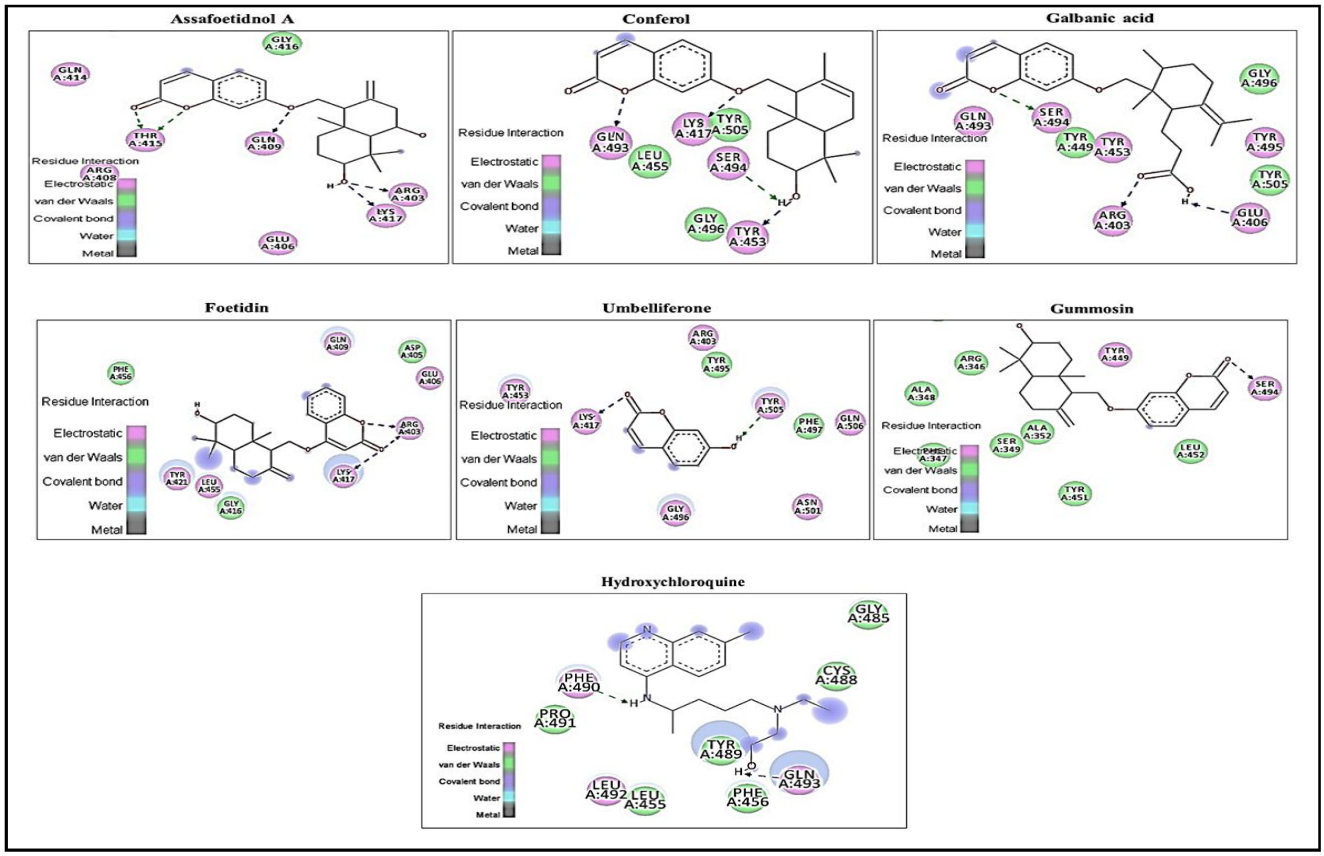

Figure 1: Docking interactions of hydroxychloroquine and sesquiterpene coumarins with SARS-CoV-2 spike glycoprotein. Hydrogen bond(s) indicated in green color; Hydrophobic bond(s) indicated in blue color.

The docking analysis of the present study explored the selective binding of sesquiterpene coumarins to the S protein binding residues of the ACE2 receptor as represented in Table 5. The selective binding of ligands to the ACE2 masks the entry point of the virus and prevents the host cell infection. In the present study, galbanic acid exhibited a stable interaction *via* forming hydrogen bonds at His34 amino acid and hydrophobic linkages at Lys353, and Arg393 with a considerable binding affinity (-3.74 kcal/mol) and inhibition constant (118.53 μM) at the RBD recognition site of ACE2 receptor. Further, conferol partly occupies ACE2 *via* forming hydrogen bond interaction with the amino acid Lys31 and hydrophobic interaction at His34 with a remarkable binding affinity (-5.96 kcal/mol) and inhibition constant (42.99 μM). Umbelliferone was also found to mask the RBD binding site of ACE2 with the binding energy -4.77 kcal/mol and an inhibition constant of 317.48 μM with two non-covalent bonds. Further, hydroxychloroquine forms 3 bond with Ser44 and Arg393 residues with a binding affinity of -4.45 kcal/mol and inhibition constant of 68.34 μM. Nevertheless, other ligands namely assafoetidinol A, foetidin, and gummosin readily abrogate RBD-ACE2 association by hydrophobic interaction (Figure 2).

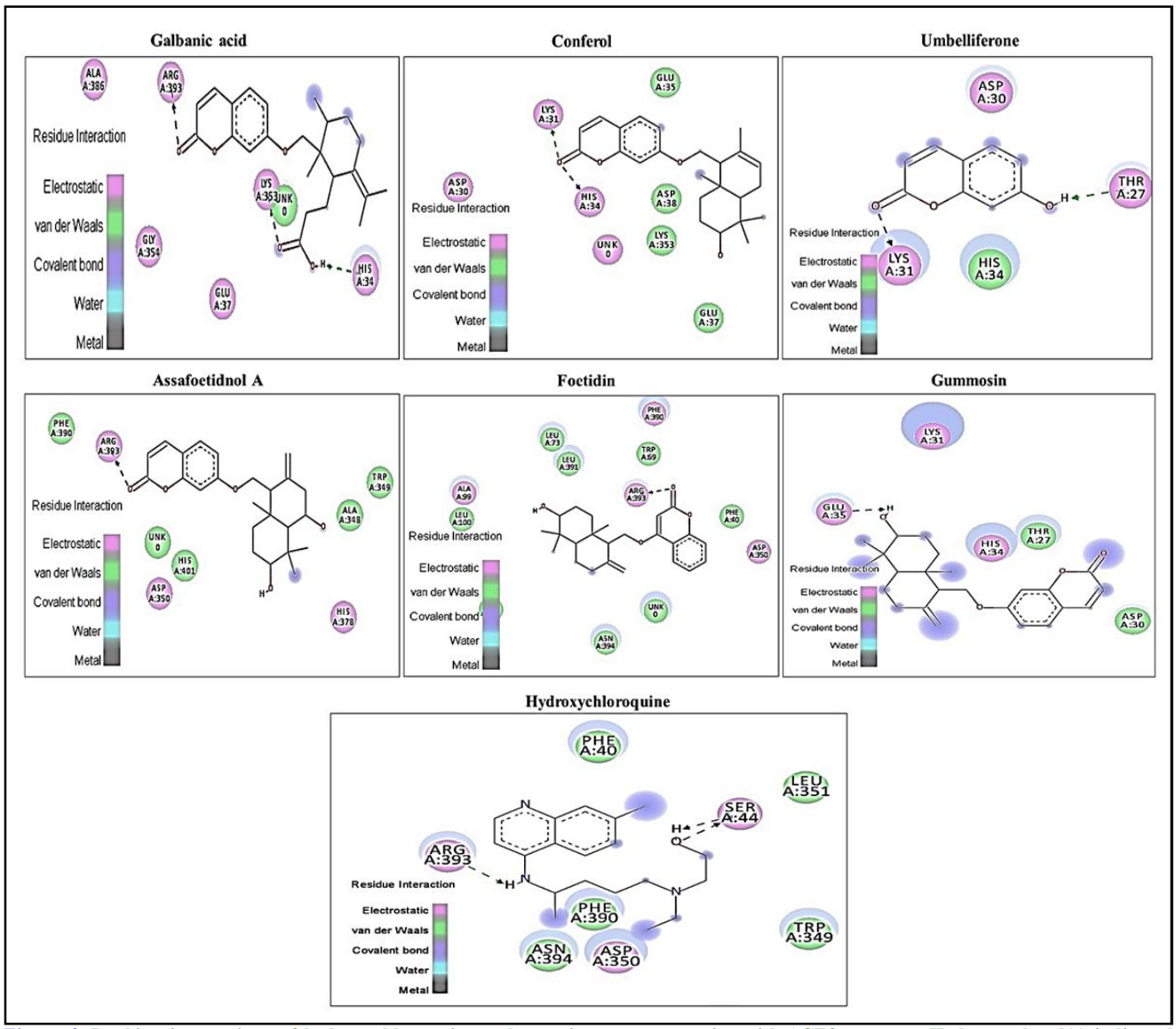

Figure 2: Docking interactions of hydroxychloroquine and sesquiterpene coumarins with ACE2 receptor. Hydrogen bond(s) indicated in green color; Hydrophobic bond(s) indicated in blue color.

3.4 *In silico* analysis of SARS-CoV-2 main protease

The selected ligands were tested with SARS-CoV-2 M^{pro} (Table 5), among them conferol showed a strong hydrogen bond interaction at catalytic site residues of Leu141, Asn142, Gly143, and hydrophobic attachment at Ser144. The binding affinity and inhibition constant of SARS-CoV-2 M^{pro} with conferol were calculated to be -7.72 kcal/mol and 2.2 μM respectively. Further, foetidin interacts with the target ligand by establishing two hydrogen bonds at Gly143 and Glu166 residues and two hydrophobic bonds at Cys155 with a binding energy of -7.44 kcal/mol and inhibition constant of 3.5 μM. All the other ligands namely gummosin, assafoetidnol A, galbanic acid, and

umbelliferone possibly interact to form hydrogen and hydrophobic bonds with a significant binding affinity and inhibition constant with the target enzyme. The stable interaction was also observed with the standard drug, hydroxychloroquine, which showed a binding affinity of -6.78 kcal/mol and inhibition constant of 152.32 µM with a stable bond at Met49 and Gly143 (Figure 3).

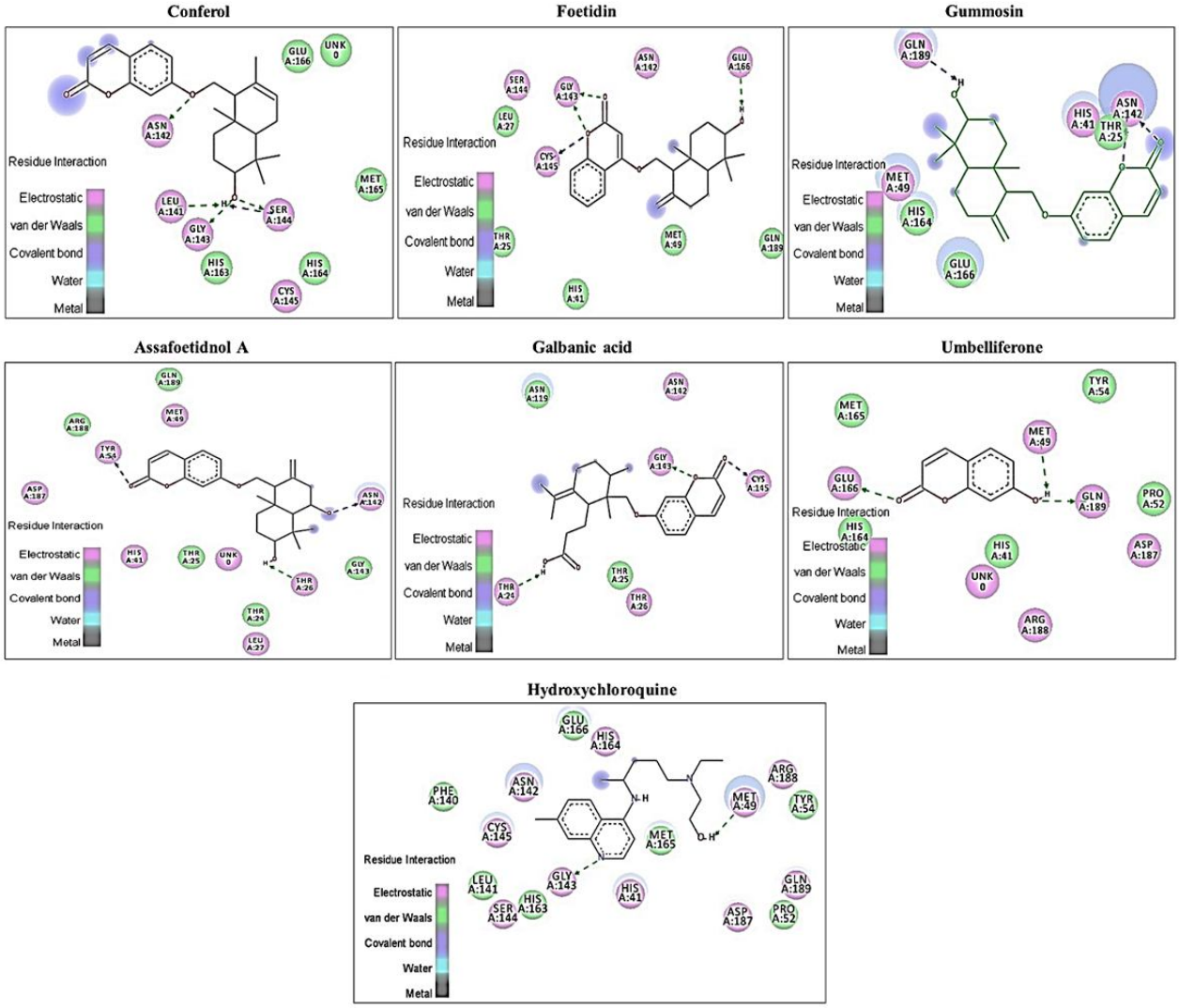

Figure 3: Docking interactions of hydroxychloroquine and sesquiterpene coumarins with SARS-CoV-2 main protease. Hydrogen bond(s) indicated in green color; Hydrophobic bond(s) indicated in blue color.

The virtual screening of papain protease exhibited a top binding score with a ligand, assafoetidnol A (Table 5). Assafoetidnol A was found to interact with the conserved active site sequences to exhibit two hydrogen bonds at Tyr268, Gln269, and two hydrophobic bonds at Tyr264, Asn267 with the binding affinity of -7.96 kcal/mol and inhibition constant of 1.45 µM. Further, ligands such as gummosin and galbanic acid were found buried individually in the active site pockets of papain protease forming a strong interaction with Tyr264, Gly266, and Gln269 residues. Nevertheless, conferol, foetidin, and umbelliferone also showed a significantly higher level of binding interaction and inhibition constant similar to hydroxychloroquine towards the activity of papain protease of COVID-19 (Figure 4).

The present study on docking analysis revealed that the umbelliferone strongly occupies the active site of RdRp *via* forming four linkages with active site residues Arg583, Ser592, Asn600 with a good docking score (-5.56 kcal/mol) and inhibition constant (547.17 µM). Further, the irreversible binding of galbanic acid with RdRp enzyme was also observed at the active site residue Lys77, Thr687 which possibly causes enzyme inhibition, which is a crucial factor for COVID-19 infection control. Assafoetidinol A also showed a stable dock score of -5.36 kcal/mol via forming two hydrophobic bonds with Asn496, Lys577, and an inhibition constant of 118.53 µM (Table 5). The virtual screening of gummosin revealed a promising binding score via occupying the catalytic domain at Arg553, Lys621 residues with a remarkable inhibitory constant. Conferol and foetidin displayed a noncovalent interaction at a single residue with considerable binding energy and inhibition constant. The standard drug, hydroxychloroquine also found to have a stable interaction at the active site of RdRp by forming 3 bonds at Gly432 and Ser433 residues (Figure 5).

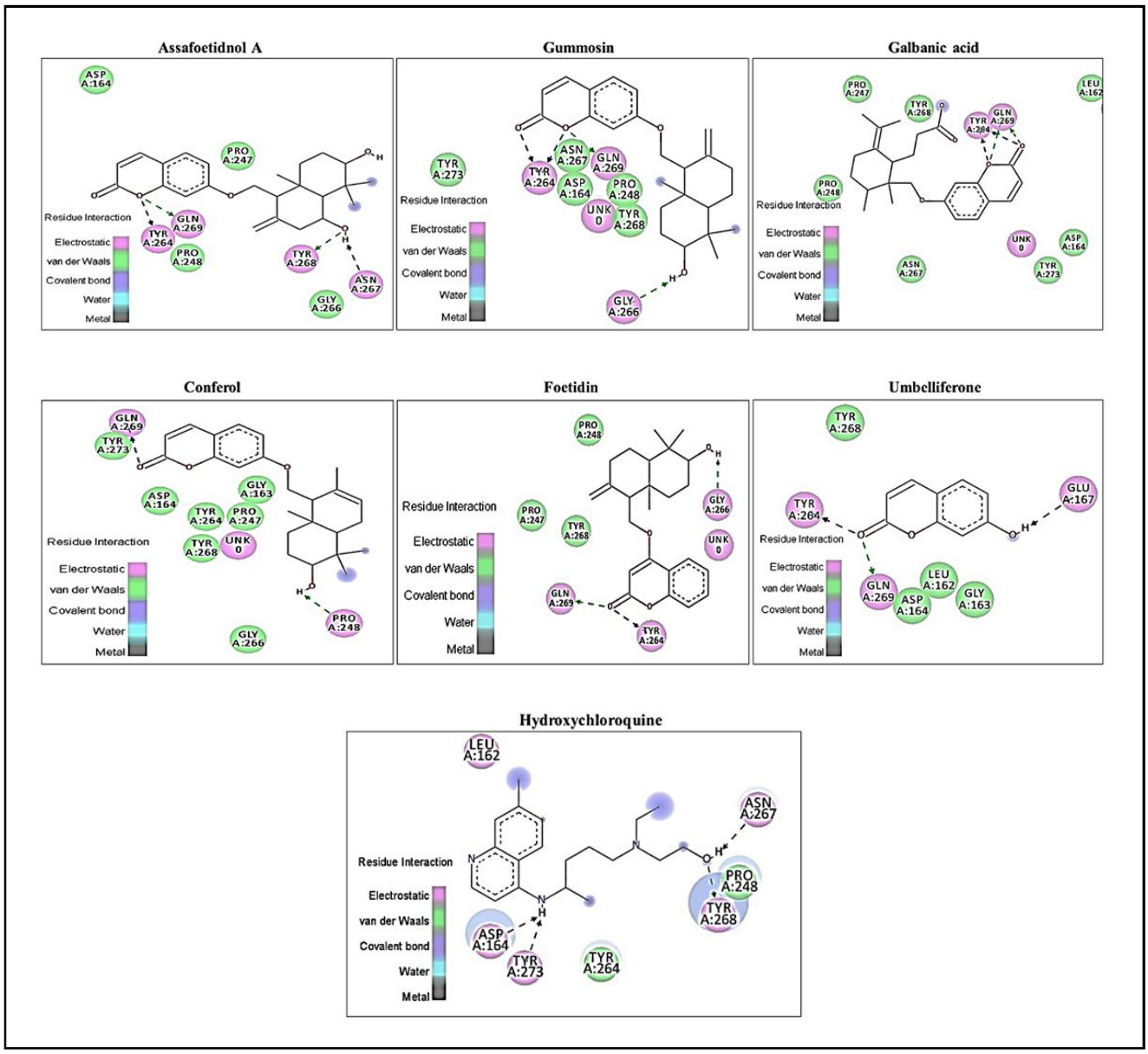

Figure 4: Docking interactions of hydroxychloroquine and sesquiterpene coumarins with SARS-CoV-2 papain protease. Hydrogen bond(s) indicated in green color; Hydrophobic bond(s) indicated in blue color.

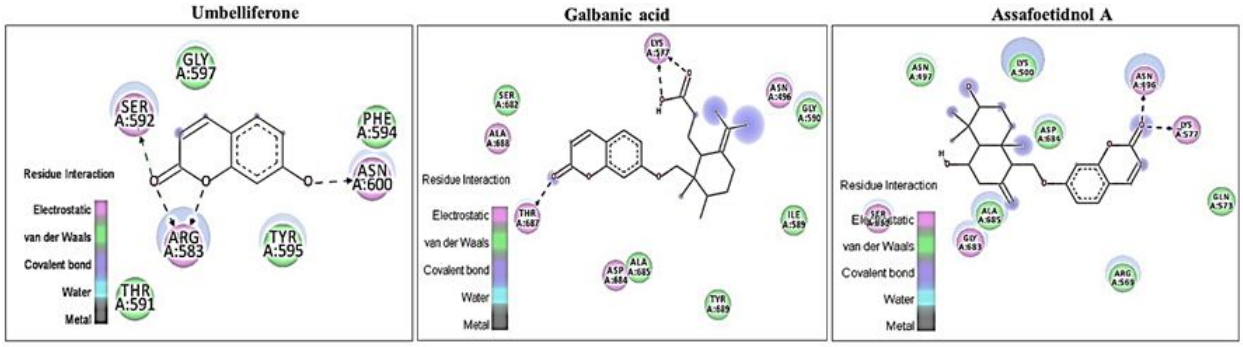

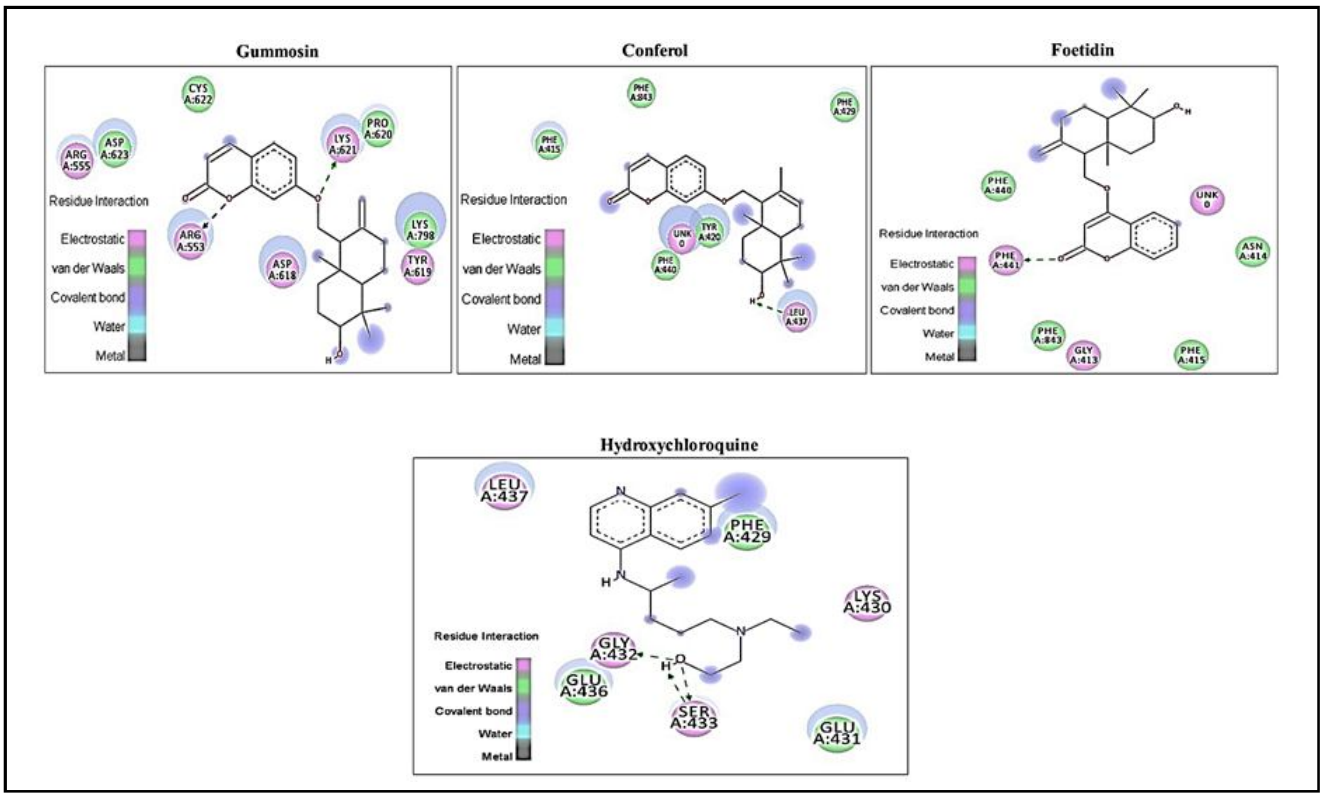

Figure 5: Docking interactions of hydroxychloroquine and sesquiterpene coumarins with SARS-CoV-2 RNA-dependent RNA polymerase. Hydrogen bond(s) indicated in green color; Hydrophobic bond(s) indicated in blue color.

Table 5: Docking interaction of hydroxychloroquine and sesquiterpene coumarins to the target proteins of SARS-CoV-2

Ligands	Binding affinity (kcal/mol)	Inhibition constant (μM)	RMSD	No. of bonds	Amino acid residues involved in hydrogen bond formation	Amino acid residues involved in hydrophobic bond formation
Spike glycoprotein RBD						
Assafoetidnol A	-5.74	61.71	357.20	5	Thr415	Arg403, Gln409, Lys417
Conferol	-6.05	36.67	359.23	4	Ser494	Lys417, Tyr453, Gln493
Galbanic acid	-5.68	68.35	355.83	3	Ser494	Arg403, Glu406
Foetidin	-5.66	70.79	354.99	3	-	Arg403, Lys417
Umbelliferone	-4.33	669.38	357.89	2	Tyr505	Lys417
Gummosin	-4.55	462.95	371.14	1	-	Ser494
Hydroxychloroquine	-3.65	196.09	370.10	2	Phe490	Gln493
ACE2 receptor						
Galbanic acid	-3.74	1.81	192.45	3	His34	Lys353, Arg393
Conferol	-5.96	42.99	189.21	2	Lys31	His34
Umbelliferone	-4.77	317.48	190.09	2	Thr27	Lys31
Assafoetidnol A	-5.94	44.05	188.09	1	-	Arg393
Foetidin	-6.83	9.86	189.04	1	-	Arg393
Gummosin	-5.39	118.53	183.00	1	-	Glu35
Hydroxychloroquine	-4.45	68.34	197.25	3	Arg393	Ser44

Main protease						
Foetidin	-7.44	3.5	23.95	4	Gly143, Glu166	Cys145
Conferol	-7.72	2.2	24.38	5	Leu141, Asn142, Gly143	Ser144
Gummosin	-7.43	3.55	25.22	3	-	Gln189, Asn142
Assafoetidnol A	-6.35	22.17	24.08	3	Thr26	Tyr54, Asn142
Galbanic acid	-5.65	72.64	23.62	3	Thr24, Gly143	Cys145
Umbelliferone	-4.74	337.83	25.38	3	Met49, Glu166, Gln189	-
Hydroxychloroquine	-6.78	152.32	23.06	2	Met49, Gly143	-
Papain protease						
Assafoetidnol A	-7.96	1.45	37.63	4	Tyr268, Gln269	Tyr264, Asn267
Gummosin	-7.7	2.28	38.90	4	Tyr264,	Gly266, Gln269
Galbanic acid	-6.01	39.18	36.15	4	Gln269	Tyr264
Foetidin	-7.25	4.86	37.18	3	Gly266, Gln269	Tyr264
Umbelliferone	-5.27	136.49	34.81	3	Gln269	Glu167, Tyr264
Conferol	-7.49	3.25	36.90	2	Pro248	Gln269
Hydroxychloroquine	-6.38	26.21	37.24	4	Tyr268	Asp164, Asn267, Tyr273
RNA-dependent RNA polymerase						
Umbelliferone	-5.56	547.17	193.35	4	Arg583, Asn600	Ser592
Galbanic acid	-5.03	204.79	186.70	3	-	Lys577, Thr687
Assafoetidnol A	-5.36	118.53	144.95	2	-	Asn496, Lys577
Gummosin	-5.06	194.4	144.52	2	Lys621	Arg553
Conferol	-5.44	102.46	181.49	1	Leu437	-
Foetidin	-4.93	241.5	185.01	1	Phy441	-
Hydroxychloroquine	-4.28	168.32	157.29	3	Gly432, Ser433	-

Docking interaction of the target protein with each ligand was represented in descending order based on the number of non-covalent interactions. RMSD-Root mean square deviation; RBD - Receptor-binding domain.

4. Discussion

Ethnopharmacological investigation of the plants exhibited knowledge of the traditional approach of natural products and their use as a potential medicine in the health care system. Natural products have long been a thriving source for the discovery of potentially active drugs against virulent targets (Shamna *et al*., 2022). The phyto-chemical exploration of asafoetida has contributed to the race for the discovery of treatment for the coronavirus disease. The present study exhibited a complementary docking approach, showing a high-performance screening of chemical components to target the resolved protein structures of COVID-19. The structure-based virtual screening methodology holds an enormous benefit in the field of drug development.

In PASS analysis, the sesquiterpene coumarins of asafoetida; namely, foetidin, umbelliferone, gummosin, conferol, assafoetidnol A, and galbanic acid expressed a broad range of biological activity, including anti-inflammatory, antiviral, and viral entry inhibitory effects when analyzed using the PASS program. Thus, these coumarins were selected and used for further investigation.

The computational method of pharmacokinetic predictions is intended to be ideal to evaluate the potency of drugs inside the living host (Moda *et al*., 2007). The selected phytocompounds were tested for pharmacokinetics proficiency, including human gastrointestinal absorption, BBB permeability, and bioavailability of the drug using SwissADME software. It has been increasing demand to develop drugs with the ability to bypass lipophilic barriers, which was attained sustainably by the lipophilic nature of the drug (Chandrasekaran *et al*., 2018). Drug lipophilicity enables positive permeation and is represented as logP/logD (Bohnert and Prakash, 2012). The present study indicated that all the drugs possess a suitable lipophilic proficiency and could cross the lipophilic biological membranes to reach the target site.

Drug permeability and solubility are two major determinants that influence the degree of gastrointestinal (GI) drug absorption (Lipinski *et al*., 2001). Interestingly, the poorly water-soluble compounds get absorbed slowly in a greater proportion in the small intestine to express pharmacological proficiency (Singh *et al*., 2018). The present study documented that compounds possess a great potential for GI tract permeability. Further, oral drug bioavailability is an outcome of the dynamic interplay of drug-likeliness behavior. Lipinski's rule of five (RO5) is used to assess the drug-likeliness of a compound possessing potential drug properties. RO5 has been widely proposed as a qualitative predictive tool to assess the absorption and

permeability properties of compounds (Lipinski, 2004). The selected sesquiterpene coumarins follows Lipinski's rule, thus indicating that the compounds were most likely regarded as potential drugs for human use.

The computational prediction of the toxicity of molecules is another essential and fundamental aspect to be assessed during drug development (Dhanya *et al*., 2018). The compound showing the least toxicity or non-toxic is always considered to be a potent and preferred drug for human consumption (Robinson *et al*., 2009). With this reference, all the sesquiterpene coumarins in this study were found to attain the least or nontoxic effect in all aspects, thus preferred as a potent ligand to act against novel coronavirus.

Globally, hydroxychloroquine, an antimalarial drug used as a potent compound to cure the symptoms of COVID-19 disease (Zafar and Snehasis, 2022). Similarly, in the molecular docking analysis, hydroxychloroquine showed a stable interaction with all the target proteins in the present study. The result of the docking parameters of hydroxychloroquine was considered as a reference and used for the comparison of the result of sesquiterpene coumarins against the pathogenic proteins of SARS-CoV-2 in the present study.

SARS-CoV-2 spike (S) glycoprotein is highly robust among all human coronaviruses (HCoVs) that helps the virus to enable receptor identification, binding, and cell membrane integration during infection (Masi Malaiyan *et al*., 2023). The receptor-binding domain of the S protein initially assists the binding of virus particles onto the surface of the entry receptor ACE2. The process of host cell invasion is possible due to the presence of specific conserved sequences in the RBD region of the S spike protein (Farag *et al*., 2023). Thus, the docking interaction of the study exposed that all the selected coumarins showed a significant binding affinity and inhibition constant with S protein RBD by forming remarkable hydrogen and hydrophobic interactions.

Several lines of research have detailed the complex interaction of virus capsid glycoprotein to the outer surface of the claw-like structure of ACE2 to initiate the pathogenic mechanism of COVID-19 (Farag *et al*., 2022). It is evident that inhibiting the receptor recognition mechanism might be a potential target to treat viral infection (Shang *et al*., 2020). An *in silico* docking analysis of all the selected compounds found to have a stable binding affinity and inhibition constant with ACE2 protein thus indicating that the coumarins of asafoetia might block the viral attachment and entry into the host cell.

In addition to the studies targeting S spike and ACE2 proteins, many studies are being conducted worldwide targeting the enzymes responsible for the virus life cycle (V'kovski *et al*., 2021; Luan *et al*., 2020). M^{pro} and PL^{pro} of SARS-CoV-2 play a fundamental role in the viral polyprotein synthesis, assembly, and spread, thus considered as a potential target to halt the COVID-19 crisis (Zhu *et al*., 2021; Anirudhan *et al*., 2021). RNA-dependent RNA polymerase (RdRp) is a key enzyme that regulates viral gene transcription and replication, thus proposed as a potential therapeutic target to inhibit viral infection (Zhu *et al*., 2020). The present study focused on the specific protein-ligand interaction of sesquiterpene coumarins with important viral proteases to hinder the process of assembly and release of viral particles within the host cell. Each specific protease enzyme has a conserved sequence at the catalytic active site where all the selected ligands were targeted. The binding of ligand was found to block the enzyme's catalytic activity, leading to enzyme inhibition. The promising docking scores were observed with all the selected sesquiterpene coumarins by irreversibly blocking the catalytic site of the main protease enzymes, thereby preventing virus multiplication and disease progression.

Although, the molecular docking provides valuable insights of potential ligand-protein interactions, the simulation of an interactions using molecular dynamics (MD) methods might describe more on the binding kinetics and stability of ligand-protein complexes. Further, the experimental validation using biochemical assays and molecular techniques are considered essential to confirm the predicted binding affinities and biological activity of sesquiterpene coumarins of asafoetida against SARS-CoV-2.

5. Conclusion

In silico molecular docking evaluation of the study concludes that all the selected sesquiterpene coumarins of asafoetida actively inhibit or modify the functional site of COVID-19 disease associated proteins, suggesting that the compounds could effectively interfere with the mechanism of the virus life cycle to reduce the virus overload and COVID-19 disease progression. Further studies are warranted to explore the anti-viral potency of coumarins to use as a potent drug to manage COVID-19 disease.

Acknowledgments

This work was supported by the Department of Biochemistry, SRM Dental College, Bharathi salai, Ramapuram, Chennai, Tamil nadu, India.

Conflict of interest

The author declares no conflict of interest relevant to this article.

References

Amalraj, A. and Gopi, S. (2016). Biological activities and medicinal properties of Asafoetida: A review. J. Tradit. Complement. Med., **7**(3):347-359.

Anirudhan, V.; Lee, H.; Cheng, H.; Cooper, L. and Rong, L. (2021). Targeting SARS-CoV-2 viral proteases as a therapeutic strategy to treat COVID-19. J. Med. Virol., **93**:2722-2734.

Bohnert, T. and Prakash, C. (2012). ADME profiling in drug discovery and development: An overview. In: Encyclopedia of Drug Metabolism and Interactions, pp:1-35.

Caly, L.; Druce, J.D.; Catton, M.G.; Jans, D.A. and Wagstaff, K.M. (2020). The FDA-approved drug ivermectin inhibits the replication of SARS-CoV-2 *in vitro*. Antivir. Res., **178**:104787.

Chandrasekaran, B.; Abed, S.N.; Al-Attraqchi, O.; Kuche, K. and Tekade, R.K. (2018). Computer-aided prediction of pharmacokinetic (ADMET) properties. In: Dosage form design parameters (ed. Tekade, R.K.), Academic Press, pp:731-755.

Daina, A.; Michielin, O. and Zoete, V. (2017). SwissADME: A free web tool to evaluate pharmacokinetics, drug-likeness and medicinal chemistry friendliness of small molecules. Sci. Rep., **7**:42717.

Dhanya, S.; Lal, K. and Reena, S.R. (2018). *In silico* toxicology : A tool for early safety evaluation of drug. J. Bioinform. Genomics Proteomics, **3**(1):1030.

Farag, M.; Pathan, A. and Aldoij, N. (2022). Molecular docking analysis of tenplant products for the inhibition of spike glycoprotein and prospective use as anti-COVID compounds. Ann. Phytomed., **11**(2):302-308.

Farag, M.; Pathan, A. and Aldoij, N. (2023). Interaction between anti-COVID compounds across spike protein subunits influences their inhibition potential. Ann. Phytomed., **12**(1):251-258.

Fehr, A.R. and Perlman, S. (2015). Coronaviruses: an overview of their replication and pathogenesis. Methods Mol. Biol., **1282**:1-23.

Kalyaanamoorthy, S. and Chen, Y.P.P. (2011). Structure-based drug design to augment hit discovery. Drug Discov. Today, **16**(17-18):831-839.

Kumar, V.; Doshi, K.U.; Khan, W.H. and Rathore, A.S. (2020). COVID-19 pandemic: Mechanism, diagnosis and treatment. J. Chem. Technol. Biotechnol., **96**:299-308.

Lipinski, C.A. (2004). Lead- and drug-like compounds: The rule-of-five revolution. Drug Discov. Today Technol., **1**(4):337-341.

Lipinski, C.A.; Lombardo, F.; Dominy, B.W. and Feeney, P.J. (2001). Experimental and computational approaches to estimate solubility and permeability in drug discovery and development settings. Adv. Drug Deliv. Rev., **46**(1-3):3-26.

Luan, B.; Huynh, T.; Cheng, X.; Lan, G. and Wang, H.R. (2020). Targeting proteases for treating COVID-19. J. Proteome Res., **19**(11):4316-4326.

Mahendra, P. and Bisht, S. (2012). *Ferula asafoetida*: Traditional uses and pharmacological activity. Pharmacogn. Rev., **6**:141-146.

Masi Malaiyan, M.; Mohan Kumar, P.; Logesh, P.; Sibi, K.; Tamizharasi, S.; Nandhakumaran, J.; Janani, S. and Prabha, T. (2023). Discovering the epigenetic pathways underlying SARS-CoV-2 infections and exploring recent epigenetic-associated clinical trials. Ann. Phytomed., **12**(2):12-20.

Moda, T.L.; Montanari, C.A. and Andricopulo, A.D. (2007). Hologram QSAR model for the prediction of human oral bioavailability. Bioorg. Med. Chem., **15**(24):7738-7745.

Naqvi, A.A.T.; Fatima, K.; Mohammad, T.; Fatima, U.; Singh, I.K.; Singh, A.; Atif, S.M.; Hariprasad, G.; Hasan, G.M. and Hassan, M.I. (2020). Insights into SARS-CoV-2 genome, structure, evolution, pathogenesis and therapies: Structural genomics approach. Biochim. Biophys. Acta Mol. Basis Dis., **1866**(10):165878.

Petersen, E.; Koopmans, M.; Go, U.; Hamer, D.H.; Petrosillo, N.; Castelli, F.; Storgaard, M.; Al Khalili, S. and Simonsen, L. (2020). Comparing SARS-CoV-2 with SARS-CoV and influenza pandemics. Lancet Infect. Dis., **20**(9):e238-e244.

Pires, D.E.V.; Blundell, T.L. and Ascher, D.B. (2015). pkCSM: Predicting small-molecule pharmacokinetic and toxicity properties using graph-based signatures. J. Med. Chem., **58**(9):4066-4072.

Poduri, R.; Joshi, G. and Jagadeesh, G. (2020). Drugs targeting various stages of the SARS-CoV-2 life cycle: Exploring promising drugs for the treatment of Covid-19. Cell. Signal., **74**:109721.

Poroikov, V.V.; Filimonov, D.A.; Ihlenfeldt, W.D.; Gloriozova, T.A.; Lagunin, A.A.; Borodina, Y.V.; Stepanchikova, A.V. and Nicklaus, M.C. (2003). Pass biological activity spectrum predictions in the enhanced open NCI database browser. J. Chem. Inf. Model., **43**(1):228-236.

Rizvi, S.M.D.; Shakil, S. and Haneef, M. (2013). A simple click by click protocol to perform docking: Autodock 4.2 made easy for non-bioinformaticians. EXCLI Journal, **12**:831-857.

Robinson, S.; Chapman, K.; Hudson, S.; Sparrow, S.; Spencer-Briggs D., Danks A., Hill, R.; Everett, D.; Mulier, B.; Old, S. and Bruce, C. (2009). Guidance on dose level selection for regulatory general toxicology studies for pharmaceuticals, London. National Centre for the Replacement, Refinement and Reduction of Animals in Research (NC3Rs), Tamworth, Laboratory Animal Science Association.

Samaddar, A.; Grover, M. and Nag, V.L. (2020). Pathophysiology and potential therapeutic candidates for COVID-19: A poorly understood arena. Front. Pharmacol., **11**:585888.

Shahrajabian, M.H.; Sun, W.; Soleymani, A.; Khoshkaram, M. and Cheng, Q. (2021). Asafoetida, God's food, a natural medicine. Pharmacogn. Commn., **11**(1):36-39.

Shamna, K.P.; Arthanari, M. and Poyi M.M. (2022). Phytocompounds in the management of COVID-19: A review. Ann. Phytomed., **11**(3):S30-S35.

Shang, J.; Ye, G.; Shi, K.; Wan, Y.; Luo, C.; Aihara, H.; Geng, Q.; Auerbach, A. and Li, F. (2020). Structural basis of receptor recognition by SARS-CoV-2. Nature, **581**:221-224.

Singh, D.; Bedi, N. and Tiwary, A.K. (2018). Enhancing solubility of poorly aqueous soluble drugs: Critical appraisal of techniques. J. Pharm. Investig., **48**:509-526.

Song, F.; Shi, N.; Shan, F.; Zhang, Z.; Shen, J.; Lu, H.; Ling, Y.; Jiang, Y. and Shi, Y. (2020). Emerging 2019 novel coronavirus (2019-nCoV) Pneumonia. radiology., **295**:210-217.

Sumathi, S. and Vidhya, S.Y. (2022). Exploiting the promising therapeutic potential of plant phytoconstituents to combat COVID-19: A review. Ann. Phytomed., **11**(3):S48-S54.

Tahir ul Qamar, M.T.; Alqahtani, S.M.; Alamri, M.A. and Chen, L.L. (2020). Structural basis of SARS-CoV-2 $3CL^{pro}$ and anti-COVID-19 drug discovery from medicinal plants. J. Pharm. Anal., **10**(4):313-319.

Tariq, A.; Mateen, R.M.; Afzal, M.S. and Saleem, M. (2020). Paromomycin: A potential dual targeted drug effectively inhibits both spike (S1) and main protease of COVID-19. Int. J. Infect. Dis., **98**:166-175.

Trougakos, I.P.; Stamatelopoulos, K.; Terpos, E.; Tsitsilonis, O.E.; Aivalioti, E.; Paraskevis, D.; Kastritis, E.; Pavlakis, G.N. and Dimopoulos, M.A. (2021). Insights to SARS-CoV-2 life cycle, pathophysiology, and rationalized treatments that target COVID-19 clinical complications. J. Biomed. Sci., **28**(9):1-18.

V'kovski, P.; Kratzel, A.; Steiner, S.; Stalder, H. and Thiel, V. (2021). Coronavirus biology and replication: implications for SARS-CoV-2. Nat. Rev. Microbiol., **19**:155-170.

Wang, D.; Hu, B.; Hu, C.; Zhu, F.; Liu, X.; Zhang, J.; Wang, B.; Xiang, H.; Cheng, Z.; Xiong, Y.; Zhao, Y.; Li, Y.; Wang, X. and Peng, Z. (2020). Clinical Characteristics of 138 Hospitalized Patients with 2019 Novel coronavirus-infected pneumonia in Wuhan, China. J. Am. Med. Assoc., **323**:1061-1069.

Zafar, S. and Snehasis, N. (2022). Molecular docking to discover potential bioextract substitutes for hydroxychloroquine against COVID-19 and Malaria. Int. J. Sci. Res., **13**(3):1571-1578.

Zhu, N.; Zhang, D.; Wang, W.; Li, X.; Yang, B.; Song, J.; Zhao, X.; Huang, B.; Shi, W.; Lu, R.; Niu, P.; Zhan, F.; Ma, X.; Wang, D.; Xu, W.; Wu, G.; Gao, G.F. and Tan, W. (2020). A novel coronavirus from patients with pneumonia in China, 2019. N. Engl. J. Med., **382**(8):727-733.

Zhu, W.; Chen, C.Z.; Gorshkov, K.; Xu, M.; Lo, D.C. and Zheng, W. (2020). RNA-dependent RNA Polymerase as a target for COVID-19 drug discovery. SLAS Discov., **25**(10):1141-1151.

Zhu, W.; Shyr, Z.; Lo, D.C. and Zheng, W. (2021). Viral proteases as targets for coronavirus disease 2019 drug development. J. Pharmacol. Exp. Ther., **378**(2):166-172.

Citation **Surekha Ramachandran (2024). Sesquiterpene coumarins of Asafoetida mask the functional site of pathogenic proteins of SARS-CoV-2 to combat COVID-19 disease. Ann. Phytomed., 13(1):495-506. http://dx.doi.org/10.54085/ap.2024.13.1.51.**